Invasive growth of *Aspergillus oryzae* in rice *koji* and increase of nuclear number

Mizuki Yasui
University of Tsukuba
Ken Oda
National research institute of Brewing
Shunsuke Masuo
University of Tsukuba
Shuji Hosoda
Tsukuba Daigaku
Takuya Katayama
University of Tokyo
Jun-ichi Maruyama
University of Tokyo
Naoki Takaya
University of Tsukuba
Norio Takeshita (takeshita.norio.gf@u.tsukuba.ac.jp)
Tsukuba Daigaku https://orcid.org/0000-0003-2666-4991

Research

Keywords: Aspergillus oryzae, koji, rice, nuclei, mitosis

Posted Date: May 19th, 2020

DOI: https://doi.org/10.21203/rs.2.22172/v2

Version of Record: A version of this preprint was published at Fungal Biology and Biotechnology on June 5th, 2020. See the published version at https://doi.org/10.1186/s40694-020-00099-9.

Abstract

Background: 'Rice *koji*' is a solid culture of *Aspergillus oryzae* on steamed rice grains. Multiple parallel fermentation, wherein saccharification of rice by *A. oryzae* and alcohol fermentation by the budding yeast occur simultaneously, lead to the formation of a variety of ingredients of Japanese sake. In sake brewing, the degree of mycelial invasive growth into the steamed rice, called '*haze-komi*', highly correlates with the digestibility and quality of rice *koji*, since the hyphae growing into the rice secrete amylases and digest starch of rice.

Results: In this study, we investigated mycelial distribution of GFP-tagged *A. oryzae* in rice *koji* made with different types of rice, such as sake rice and eating rice, with 50 or 90% polishing rate to remove abundant proteins and lipids near the surface. In addition, we compared transcriptomes of *A. oryzae* in the different types of rice *koji*. Finally, we found that *A. oryzae* increases the nuclear number and hyphal width in the course of 1-3 days cultivation.

Conclusions: Our imaging analyses indicate that *A. oryzae* hyphae grew more deeply into 50% polished rice than 90% polished rice. The increases of nuclear number may be a selectively acquired characteristic for the high secretory capacity during the breeding in long history.

Introduction

Filamentous fungi secrete a variety of enzymes to degrade extracellular organic compounds, serving as decomposer in nature (1). In addition, modern biotechnologies have utilized filamentous fungi as cell factories for the production of organic acids, drugs including antibiotics and enzymes due to high secretory capacity (2). Fungal biotechnology plays a central role for many industries such as food and feed, pharma, detergent, bio-fuel and etc. Filamentous fungi grow by hyphal tip growth, forming multi-cellular networks with branching cells at subapical regions (3-5). Hyphae and mycelial networks are specifically adapted for growing on solid surfaces and invading substrates and tissues (6).

The filamentous fungus *Aspergillus oryzae* has been used in the production of traditional fermented foods such as sake (rice wine), miso (soybean paste) and shoyu (soy sauce) for more than 1,000 years in Japan (7). The safety of *A. oryzae* is guaranteed by the long history of use in food fermentation industries and molecular genomic and metabolomic analyses (8, 9), which is supported by the World Health Organization (10). *A. oryzae* has been used commercially as a host for homologous and heterologous protein production as well in modern biotechnology (11, 12). One of the distinctive features in the use of *A. oryzae* in Japanese traditional fermentation is the use of solid-state cultivation (rice grain, soybean and wheat bran). Since filamentous fungi often secrete more enzymes in solid-state culture than in submerged culture (13-15), several commercial enzymes are produced in solid-state culture in addition to traditional fermentation methods. For example, glucoamylase and acid protease encoding genes, *glaB* and *pepA*, respectively, are known as the solid-state-specific genes of *A. oryzae* (16-18). Transcriptome

and proteome analyses have revealed the ability of *A. oryzae* to produce heterologous proteins in solid-state culture (15, 19).

'Rice *koji*' is a solid culture of *A. oryzae* on steamed rice grains. Multiple parallel fermentation, wherein saccharification of rice by *A. oryzae* and alcohol fermentation by the budding yeast (*Saccharomyces cerevisiae*) occur simultaneously, lead to the formation of a variety of ingredients in Japanese sake with its characteristic tastes. Sake contains more than 280 metabolites that affect its quality. The metabolite composition of sake depends on the combination of raw materials and sake-making parameters (e.g., rice races, rice polishing ratio, water quality, *koji* mold, yeast strains, sake mash fermentation methods) used during manufacturing (20). In sake brewing, the degree of hyphal penetration into the steamed rice, called '*haze-komi*', highly correlates with the digestibility and quality of *koji* (21-25), since the hyphae growing into the rice secrete amylases and digest the starch. The *haze-komi* is believed empirically to determine the distribution and composition of enzymes in rice *koji*, the step of fermentation and the qualities of sake. Recently, the hyphal penetration into steamed rice was visualized by b-glucuronidase (GUS)-expressing *A. oryzae* (26). The correlation with the spread of glucose during fermentation was shown by mass spectrometry imaging (MSI) of glucose (26).

Japanese people normally consume eating rice as food, while sake is made with sake rice, which is especially suitable to sake brewing. Features of sake rice are large grains generally with "white core"(or *shinpaku* in Japanese), a low protein content and high solubility during the brewing process, which facilitates *A. oryzae* invasive growth (27). Distribution of nutrients in a grain of rice is not uniform. Proteins and lipids are abundant near the surface of rice, resulting in miscellaneous taste and off-flavor of sake (28). The Japanese high-quality sake, *daiginjo-shu*, is made from highly polished rice with polishing ratio less than 50% (29).

In this study, we investigated mycelial distribution using GFP-tagged *A. oryzae* in rice *koji* made with different types of rice (sake rice or eating rice, 50 or 90% polishing ratio).

Materials And Methods

Rice and fungal species. *Yamada-nishiki* (sake rice) and *Chiyo-nishiki* (eating rice) were used to make *koji*. The rice grains were polished to different ratios (50% and 90%) using a milling machine (HS-08CNC, Chiyoda, Hiroshima, Japan). 90% polishing rate means polishing 10% outside of rice. *Yamada-nishiki* and *Chiyo-nishiki* with polished rate 50% or 90% are referred as Y50, Y90, C90, respectively. The H2B ORF was amplified from the genomic DNA of *A. oryzae* wild strain RIB40 using the primers PamyB-H2BF: 5'-TCGAGCTCGGTACCCATGGCACCCAAGGCTGCTGA-3', Tag-H2BR: 5'-CAAGAAAGCTGGGTCCCCTTTGGCAGAAGAGGAGTACTTCGTA-3' and then ligated with the SmaI-digested pUtNAN (30), yielding the plasmid pUtH2BG. The NotI-digested pUtH2BG was introduced into the RIB40Δn strain (31), yielding the strain RIB40UtH2BG expressing H2B-GFP. *A. oryzae* strain RIB40UtH2BG (pUtH2BG) was used to make *koji*.

Small-scale *koji* making. 2-5 g of the rice were soaked in water until the weight increased 30%; Y50 for 6 min 40 sec, Y90 and C90 for 120 min. They were steamed for 10 min in a steamer, then keep the lid of steamer closed for 15 min after turning off the heat. The steamed rice was inoculated with spores of *A. oryzae*, 10^4 spores per rice 1 g, and incubated in lab dishes with papers containing 4 ml water to keep humidity at 30^{o}C for 33 h. Temperature of the incubator was raised to 42^{o}C gradually for 15 h, total 48 h.

Rice *koji* sectioning. One grain of rice *koji* was embedded with the optimal cutting temperature compound (Sakura-finetech, Japan) in a mold, and frozen at -80^{o}C. The frozen sample block was sectioned by using a cryostat (CM1850, Leica microsystems). Longitudinal sections with 30 mm thickness were obtained from the approximate center of the rice *koji.* Adhesive film was used to acquire the sample sections. Chamber and sample holder temperatures were kept at -20^{o}C. The sections were placed on a glass slide for imaging analysis.

Microscopes. The confocal laser scanning microscope (CLSM) LSM880 (Carl Zeiss, Jena, Germany) equipped with a 63×/0.9 numerical aperture Plan-Apochromat objective was used to acquire confocal microscopic images. We visualize fungal and rice cells by CLSM and confocal reflection microscopy. Fungal nuclei and rice cells were visualized with 488 and 400-nm lasers, respectively. Acquired confocal images were analyzed using ZEN Software (Version 3.5, Carl Zeiss) and ImageJ software. Another CLSM TCS SP5 (Leica, Mannheim, Germany) equipped with HC PL APO 20x/0.75 IMM CORR CS2 objective lens was used to acquire confocal dual-color microscopic images. Epi-fluorescent inverted microscopy; Cells were observed by Axio Observer Z1 (Carl Zeiss) microscope equipped with a Plan-Apochromat 63 × 1.4 Oil or 10 or 20 times objective lens, an AxioCam 506 mono camera and Colibri.2 LED light (Carl Zeiss). Temperature of the stage was kept at 30°C by a thermo-plate (TOKAI HIT, Japan). Zoom microscopy; Plates were observed by AXIO Zoom V16 and HXP 200C illuminator (Carl Zeiss). Images were collected and analyzed by using the Zen system (Carl Zeiss) and ImageJ software.

SEM. Benchtop Scanning Electron Microscope JCM-6000 (JEOL, Japan) was used to observe *koji* section cut by a scalpel in low vacuum condition without special treatment.

Transparentizing of rice. We made rice tissues of rice koji transparent according to the attached protocol of tissue-clearing reagent TOMEI (Tokyo Chemical Industry, Japan). One grain of rice *koji* was soaked in PFA at room temperature in the dark for 30 min. The PFA was replaced with PBS and incubated for 5 min, then washed three times by incubating for 10 min with new PBS. The rice *koji* was incubated in 10, 30, 50, 70, 100% TOMEI regent (2,2'-Thiodiethanol containing Propyl Gallate, PBS and DMSO) for 10 min respectively. The sample in TOMEI regent was used for imaging analysis.

X-ray CT. Mycelia in the rice *koji* are detected by an X-ray CE, SMX-160CTS (Shimadzu). One grain of rice *koji* was placed on the rotary table between the X-ray tube and the X-ray detector, and rotated to collect X-ray data from all angles. The volumes of mycelia are calculated by VG Studio MAX software.

RNA-seq analysis. To isolate the total RNA from fungal cells in rice *koji*, rice *koji* was frozen and homogenized using mortar and pestle, and then the total RNA was extracted using an RNA isolation kit

(RNA Mini Kit, Zymo Biomics). Novogen Inc. supports library preparation, sequencing and partial data analysis. Each sample is sequenced using 150-bp paired-end reads on an Illumina NovaSeq 6000 instrument. The reads are mapped to reference genomes of *A. oryzae* RIB40, NCIB ID: 510516, through CLC Genomic Workbench (QIAGEN). After log2 transformation of RPKM+1 and quantile normalization, differentially expressed genes were selected on conditions of log2 > 2 in expression level. The dataset of RNA-seq was deposited at DDBJ Sequence Read Archive (DRA) under the accession DRA009542.

Results

Imaging analysis of *A. oryzae* penetration into steamed rice.

Yamada-nishiki (sake rice) and *Chiyo-nishiki* (eating rice) were polished to 50% or 90% (removed 10% outside), and used to make *koji*, the steamed rice with *A. oryzae* mycelia (see Materials and methods), referred as Y90, C90 and C50, respectively (Fig. 1A). *A. oryzae* mycelia grew on and in the *koji* pellets. We observed surfaces and cross sections of *koji* pellets by a zoom microscopy (Fig. 1A, B). To evaluate the degree of invasive growth into the steamed rice, called '*haze-komi*', we used the *A. oryzae* strain, in which histone H2B are labeled with GFP, to make *koji*. The *koji* was sliced in 30 mm sections using a cryomicrotome. The sections were observed by a fluorescent microscopy. High intensity of GFP signals covered the periphery of rice in the Y90, C90 and C50 *koji* (Fig. 1C). Moreover, we could detect each hypha with GFP signal at cellular level in the rice. We quantified the *haze-komi* by measuring how far hyphae penetrated from the *koji* surface in the Y90, C90 and C50 (Fig. 1D, Supplemental figure 1A). The hyphal lengths from the *koji* surface in C90 and Y90 were comparable, 371 $\pm$ 60 and 311 $\pm$ 38 mm, respectively (n = 20 hyphae in 3 independent *koji*). Notably, the hyphae in Y50 penetrated more deeply 1.4 - 1.6 times, 501 $\pm$ 66 mm (n = 20 hyphae in 3 independent *koji*). There was no clear difference in the GFP intensities on the surface between the different types of rice.

A. oryzae penetration inter-rice cells and intra-rice cells.

In the *koji* sections, rice endosperm cells were observed in bright field and UV light irradiation as well due to the autofluorescence (Fig. 2A). GFP signal from *A. oryzae* often indicated similar patterns with rice cells, suggesting that hyphae often grow between rice cells, which is consistent with the previous report (32). In addition, higher magnification images showed hyphal growth inside of rice cells (Fig. 2A arrows, Supplemental figure 1B). Confocal microscopy imaging of the *koji* sections confirmed that hyphae grew inside of rice cells and frequent co-localization of fungal signal on outlines of rice cells (Fig. 2B, Movie 1 and 2, Supplemental figure 1C). The hyphal growth inter-rice cells and intra-rice cells were observed similarly in the Y90, C90 and C50.

We tested the chemical reagent TOMEI (see Materials and methods), that turns plant tissues transparent, for the *koji*. Confocal imaging visualized network-like GFP signal from *A. oryzae* co-localized with the arrangement of rice cells (Fig. 2C).

SEM analysis of *A. oryzae* penetration intra-rice cells.

We observed the cross sections of *koji* by fluorescent microscopy and found that some hyphae grew through surrounding space like a furrow in the rice (Fig. 3A, arrow and dotted line). Scanning Electron Microscopy (SEM) also indicated the hyphae in furrows on the rice cross sections (Fig. 3B, white arrows), although the shapes of rice cells were not clearly observed. The SEM imaging showed that some hyphae came from or went into a hole on the rice cross sections (Fig. 3B, yellow arrows). The holes and furrows appeared to be tunnels formed by the sugar degradation during the hyphal growth in rice cells, which is in agreement with the previous report (33).

Time-lapse imaging of *A. oryzae* penetration into steamed rice.

To monitor the time course of *A. oryzae* growth into the steamed rice, we applied fluorescent live imaging for the cross sections of *koji* Y50 and Y90 (Fig. 4). The conidia were inoculated on the surface of rice, then the *koji* was incubated for 7 hours. Z-stack images of the cross sections were taken every 10 or 20 min for 14 hours. The Z-stack merged images were shown by time-lapse movies (Movie 3, 4). We could visualize *A. oryzae* hyphae (green) penetration into the steamed rice (red), which is termed *haze-komi*, by live imaging (Fig. 4). In Y50, hyphae grew from the surface of rice towards the center of rice (Fig. 4A, B). While some hyphae grew through the rice cell shape, others changed the growth direction when they bumped against rice cells (arrows). The hyphae appeared to grow on the outside rice surface following the growth into the rice. In Y90, hyphal signal increased under the surface of rice (Fig. 4C, D). In contrast to Y50, most hyphae did not continue to penetrate towards the center of rice but grew close to the surface, mainly ~300 mm, with more branching than in Y50.

X-ray CT analysis of *A. oryzae* penetration into steamed rice.

To complement fluorescence microscopy results and obtain more accurate information on mycelial penetration into the steamed rice, we performed a X-ray CT (Computed Tomography) scan analysis (see methods). The intact C90, Y90 and Y50 incubated for 48 hours were set in the X-ray CT device, respectively. The X-ray CT scan produces cross-sectional tomographic images by use of computer-processed combinations of many X-ray measurements taken from different angles, allowing to observe the inside of objects without cutting. The 3D section images were shown by sequence images (Fig. 5A). The fungal signals were determined by the different peak found in CT value (X-ray absorption) line profiles between the *koji* (rice + *A. oryzae*) and the rice without the fungus (Fig. 5B). The rice and fungal mycelia are shown in white and yellow, respectively (Fig. 5A, Movie 5-7). In the C90 and Y90, the fungal signals were detected mainly close to the surface of rice. In the Y50, in contrast, the signals were detected both close to the surface and inside of rice.

The rice and fungal volumes were calculated from the 3D data. The ratios of fungal volume per *koji*, rice + fungus, volumes were indicated in C90, Y90 and Y50 (Fig. 5C). The fungal ratios in the C90 and Y90 were 0.44 ± 0.02, 0.32 ± 0.03, respectively, while the fungal ratio in the Y50 was 0.67 ± 0.1 and significantly higher than those in the C90 and Y90, ($n = 3$, $p \leq 0.001$). The X-ray CT scan analysis also supports deeper invasive growth in the Y50 than the C90 and Y90.

Transcriptome analysis

We compared the transcriptome profiles of *A. oryzae* in Y50, Y90 and C90 by RNA-seq analysis. The effects of the variety of rice and the polishing rate on the growth of *A. oryzae*, enzyme production, and metabolism production in *sake-koji* have been investigated previously (34). One of the most important roles of *A. oryzae* in rice *koji* is the supply of enzymes, vitamins, nutrition, such as glucose, amino acids and peptides, that are necessary for sake brewing. From the viewpoint, we compared the expression of genes (Supplemental Table 1). Especially, the comparison between Y50 and Y90 was summarized in Table 1. Digestion of starch and supply of glucose by amylases are the basis of alcohol fermentation. The expression of genes for a-amylases (*amyA, amyB* and *amyC*) and glucoamylase (*glaA*) was 5.2 and 1.7 times higher in Y50 than in Y90, whereas the expression level of maltases, which hydrolyse maltose to glucose, was comparable. The metabolic genes in glycolysis, TCA cycle and electron transport chain were compared by a heatmap (Supplemental figure 2).

Acid proteases are involved in the digestion of the main protein of rice glutelin, also called oryzanin. The enzyme breaks down the protein body containing glutelin, resulting in disruption of the rice structure. Carboxypeptidases degrade peptides and supply amino acids. The expression of major acid protease gene, *pepA,* was 13 times lower in Y50 than that in Y90, whereas the expression level of carboxypeptidase genes was almost unchanged.

The outer surface of rice, aleurone layer, is rich in lipids and fatty acids, and thier contents decreases as the polishing rate decreases (35). When the polishing rate decreases, the ratio of saturated fatty acids and unsaturated fatty acids changes (35). In sake brewing, fatty acids are important in the production of yeast-derived aroma components (*ginjo* aroma, especially ethyl caproate). When the unsaturated fatty acid content increases, the production of ethyl caproate in yeast is suppressed. The secreted lipase is necessary for supplying lipids and fatty acids to yeast. The expression of fatty acid synthase genes, *fasA and fasB*, was 5-7 times higher in Y50 than those in Y90. Additionally, the expression of *sdeA and sdeB* genes for delta-9-stearic acid desaturase, which converts palmitic acid and stearic acid to palmitoleic acid and oleic acid, respectively, was 13-20 times higher in Y50 than Y90, whereas the expression level of lipase genes was almost unchanged.

Supply of phosphate affects the following yeast fermentation (36). Phytic acid is a preserved state of phosphate in plants, and its content decreases as the rice polishing rate decreases (35). Phytases function to release phosphate from phytic acid (37). The expression of phytases, acid phosphatases and alkaline phosphatases tend to increase in Y50 compared to Y90.

Most of sake yeasts lack some of the genes related to vitamin biosynthesis. In addition, enzymes involved in fermentation require vitamins as cofactor. Supply of vitamins from *koji* is essential to proceed with fermentation (38). Vitamins are abundant in the outer surface layer and germ of rice, and their amounts decrease as the rice polishing rate decreases (39). The expression of synthesis genes for thiamine, pantothenate and biotin (Vitamin B1, 5 and 7, respectively) increased in Y50 compared to Y90.

Beside the genes related to brewing and fermentation, genes for conidiophore development, *flbA-D* and *brlA* (40), were up-regulated in Y50 compared to Y90, whereas *abaA,* which is required for phialide differentiation, was unchanged. In *A. oryzae*, *flbC* was reported to regulate the expression of genes specifically under solid-state cultivation conditions, possibly independent of the conidiation regulatory network (41).

Increase number of nuclei in *A. oryzae* hyphae

We observed nuclei labeled with GFP of *A. oryzae* in the *koji* and found that the number of nuclei often varied in each hypha (Supplemental figure 3). Since the increase of nuclei in *A. oryzae* was predicted to be correlated to the high secretion capacity of several enzymes, we focused on the phenotype. The nuclear distribution in *A. oryzae* has been analyzed in hyphae and especially in conidia (42, 43), which indicated multi-nuclear conidia; the number of nuclei in each conidium varied from 1 to 7 in *A. oryzae* strains used in sake brewing. We investigated the nuclear distribution in *A. oryzae* hyphae grown in detail by using the minimal medium but not the rice *koji*. Some of hyphae contained less than 20 nuclei in the tip compartments, the hyphal cell from the tip to the first septum (Fig. 6A, upper). Other hyphae contained more than 200 nuclei in the tip compartments (Fig. 6A, lower). The hypha containing such a high number of nuclei was imaged by the Z-stack confocal microscopy and shown in 3D imaging (Fig. 6B, Movie 8).

We classified the pattern of nuclear distribution into three types as follows. Class I; nuclei distribute at a constant interval without overlapping. Class II; nuclei align but sometimes overlap. Class III; nuclei scatter over through hyphae but not align. We counted the ratios of class I-III in the time course at 24-, 48- and 72-hours growth (Fig. 6C). At 24 hours, class II was large, while class I and III were approximately 20%. At 48 and 72 hours, class III increased to 60% and more than 70%, respectively. The class III hyphae were usually thicker than those of class I. We measured the hyphal width at tip compartments at 24-, 48- and 72-hours of growth (Fig. 6D). At 24 hours, the hyphal width was 3 to 6 mm. At 48 hours, the ratio of 7 to 10-mm hyphae increased, then at 72 hours, the hyphal width ranged 3 to 12 mm.

As a comparison, we investigated the nuclear distribution in the model fungus *Aspergillus nidulans* as well in the same way. The ratios of class I and II did not vary approximately 40% and 60%, respectively, in the time course at 24-, 48- and 72-hours (Fig. 6C). The hyphal widths were comparable at 24 and 48 hours, then the peak shifted by 2 mm wider at 72 hours (Fig. 6D). These results indicate that *A. oryzae* increases the nuclear number and hyphal width in the time course of 1-3 days, which may correlate with the high secretory capacity of several enzymes.

Synchronous mitosis in *A. oryzae*

To analyze the mechanism of the increase in nuclear number, we investigated the nuclear distribution in mitosis. Synchronous nuclear division in a hyphal compartment has been known in *A. nidulans* (44-46). We used the *A. nidulans* strain expressing NLS of the TF StuA tagged with GFP (45,47). The GFP protein localizes in nuclei in interphase, while they move out from the nuclei to cytoplasm due to partial disassembly of nuclear pore complex during closed mitosis (Fig. 7A, Movie 9) (46, 48). The nuclear

membrane envelope is intact but permeable, known as partially open mitosis. After mitosis, GFP signals moved back in the two-fold number of nuclei.

We investigated the nuclear distribution in *A. oryzae* mitosis, where histone H2B labeled with GFP remained in nuclei during mitosis. Time-lapse imaging revealed the synchronized mitosis within 5 min in the tip compartment (Fig. 7B, Movie 10). Even in the class III hypha, a lot of nuclei divided within 5 min in the tip compartment (Fig. 7C, Movie 11). We performed Z-stack and time-lapse of the class III hyphal mitosis and revealed the synchronized mitosis, although the time and space resolutions were not sufficient to demonstrate all nuclei enter mitosis at same time, Movie 11 showing that the H2B-GFP signals undergo condensation simultaneously suggests a synchronous nuclear division (49). The nuclei moved a lot after mitosis in *A. oryzae* which is consistent with that in *A. nidulans* (48). Since the size of the H2B-GFP signal did not show significant difference from 24 to 72 hours, 2.5 $\pm$ 0.3 and 2.5 $\pm$ 0.2 mm (n=10 from Movie 10 and 11), the increase in nuclear number is not due to fragmentation of nuclei.

The nuclear distribution in class III hypha of *A. oryzae* resembles that of the another model fungus *Neurospora crassa* (Fig. 7D, Movie 12, 13), whose mitosis is not clear to be synchronous or not (50).

Discussion

We improved the base of imaging analyses to evaluate '*haze-komi*', fungal penetration into steamed rice, by using a fluorescent microscopy. Our analyses indicate that *A. oryzae* hyphae grew more deeply into 50% polished rice Y50 than 90% polished rice Y90 and C90. Since proteins and lipids are abundant near the surface in a grain of rice (27), the 50% polished rice consists of mainly starch. It is likely that *A. oryaze* mycelia grow near the surface in 90% polished rice due to sufficient supply of nutrients near the surface, while the mycelia grow deeply into 50% polished rice to search for nutrients and water as well. That is believed by experience of sake brewers as evaluated by several methods (22-25), which correlates with our results. We visualized fungal hyphae in cellular level in rice *koji*. Our data support that hyphae penetrate between rice cells and grow inside of rice cells. These imaging analyses are widely applicable by proper staining for rice *koji* using different *A. oryaze* strains, different rice races and polished rates. These approaches contribute to monitoring the status and quality of rice *koji* and to screening the combination of *A. oryaze* strains and rice races according to favored qualities of sake.

Another important finding is that *A. oryzae* increases the nuclear number drastically, 20 to more than 200 nuclei in the hyphal tip compartment. The increase of nuclear number is correlated with the hyphal width. The hyphal growth did not slow down at 72 hours, in addition septation sites were usual. The hyphal tip compartments contain more nuclei at higher density. That phenomenon was not observed in *A. nidulans* (Fig. 6) and has not been reported in other filamentous fungi. One of the reasons that could explain the increase of nuclear number was that mitosis is not synchronized, resulting in gradual increase of nuclear number. Asynchronous nuclear division cycles are known in *Ashbya gossypii* (51), which is a filamentous fungus closely related to the budding yeast *S. cerevisiae*. We found, however, that a lot of nuclei even in the class III hypha of *A. oryzae* divided synchronously (Fig. 7B, C). Another possibility is a defect in cell

cycle checkpoint at G1/S transition (52). Cellular size is usually maintained by the checkpoint at G1/S transition of cell cycle, which represses the mitosis until the cell grows to a proper size. The cellular size in *A. oryzae* increased in the time course of 1-3 days, which might be caused by any defect in the G1/S checkpoint. That might allow the increase of nuclear number in the larger cell, however, the mechanism remains unknown. The increase of nuclear number in *A. oryzae* is likely correlated with the secretory capacity of several enzymes. The characteristic could be an extremely important feature of *A. oryzae.* Since the increase of nuclear number is not clearly observed in closely related species *A. flavus* (unpublished data), the characteristic may be a selectively acquired character during a long history brewing. Next assignment will be the molecular mechanism of increased nuclear number in *A. oryzae* and possibility for application in.

Conclusion

Our imaging analyses indicate that *A. oryzae* hyphae grew more deeply into 50% polished rice Y50 than 10% polished rice Y90 and C90. Another important finding is that *A. oryzae* increases the nuclear number drastically, 20 to more than 200 nuclei in the hyphal tip compartment. The increases of nuclear number may be a selectively acquired characteristic for the high secretory capacity during the breeding in long history.

Declaration

Acknowledgments

This work was supported by NIMS microstructural characterization platform (NMCP) as a program of "Nanotechnology Platform" of the Ministry of Education, Culture, Sports, Science and Technology (MEXT), Japan. We are grateful to Akiko Takenouchi in NMCP for technical assistant of X-ray CT, grateful to Li Xianglan for technical assistant of cryostat.

Funding

This work was supported by Japan Society for the Promotion of Science (JSPS) KAKENHI grant number 18K05545, Noda Institute for Scientific Research Grant and Japan Science and Technology Agency (JST) ERATO grant number JPMJER1502.

Authors' contributions

N.T. and N.T. designed the research project. M.Y., S.H. and N.T. performed microscopy experiments and analyzed the data. M.Y., K.O. and S.M. performed RNA-seq and analyzed the data. T.K. and J.M. constructed the plasmid and *A. oryzae* strain. M.Y., K.O. and N.T. wrote the paper with inputs from other coauthors.

Availability of data and materials

The dataset of RNA-seq was deposited at DDBJ Sequence Read Archive (DRA) under the accession DRA009542.

Abbreviations

Not Applicable.

Ethics approval and consent to participate

Not applicable.

Consent for publication

Not applicable.

Competing interests

The authors declare that they have no competing interests.

References

1. Klein DA, Paschke MW. Filamentous fungi: the indeterminate lifestyle and microbial ecology. Microb Ecol. 2004;47:224-35.
2. Meyer V, Andersen MR, Brakhage AA, Braus GH, Caddick MX, Cairns TC, de Vries RP, Haarmann T, Hansen K, Hertz-Fowler C, Krappmann S, Mortensen UH, Peñalva MA, Ram AFJ, Head RM. Current challenges of research on filamentous fungi in relation to human welfare and a sustainable bio-economy: a white paper. Fungal Biol Biotechnol. 2016;3:6.
3. Riquelme M, Aguirre J, Bartnicki-García S, Braus GH, Feldbrügge M, Fleig U, Hansberg W, Herrera-Estrella A, Kämper J, Kück U, Mouriño-Pérez RR, Takeshita N, Fischer R. Fungal morphogenesis, from the polarized growth of hyphae to complex reproduction and infection structures. Microbiol Mol Biol Rev. 2018;82:1-47.
4. Takeshita N. Coordinated process of polarized growth in filamentous fungi. Biosc Biotech Biochem. 2016;80:1693-1699.
5. Takeshita N, Evangelinos M, Zhou L, Serizawa T, Somera-Fajardo RA, Lu L, Takaya N, Nienhaus GU, Fischer R. Pulses of Ca2+ coordinate actin assembly and exocytosis for stepwise cell extension. Proc Natl Acad Sci U S A. 2017;114:5701-5706.
6. Hölker U, Höfer M, Lenz J. A survey of computational and physical methods applied to solid-state fermentation. Appl Microbiol Biotechnol. 2004;65:9-17.
7. Machida M, Yamada O, Gomi K. Genomics of *Aspergillus oryzae*: learning from the history of *Koji* mold and exploration of its future. DNA Res. 2008;15:173-83.
8. Barbesgaard P, Heldt-Hansen HP, Diderichsen B. On the safety of *Aspergillus oryzae*: a review. Appl. Microbiol. Biotechnol. 1992;36:569-572.

9. Machida M, Asai K, Sano M, Tanaka T, Kumagai T, Terai G, Kusumoto K, Arima T, Akita O, Kashiwagi Y, Abe K, Gomi K, Horiuchi H, Kitamoto K, Kobayashi T, Takeuchi M, Denning DW, Galagan JE, Nierman WC, Yu J, Archer DB, Bennett JW, Bhatnagar D, Cleveland TE, Fedorova ND, Gotoh O, Horikawa H, Hosoyama A, Ichinomiya M, Igarashi R, Iwashita K, Juvvadi PR, Kato M, Kato Y, Kin T, Kokubun A, Maeda H, Maeyama N, Maruyama J, Nagasaki H, Nakajima T, Oda K, Okada K, Paulsen I, Sakamoto K, Sawano T, Takahashi M, Takase K, Terabayashi Y, Wortman JR, Yamada O, Yamagata Y, Anazawa H, Hata Y, Koide Y, Komori T, Koyama Y, Minetoki T, Suharnan S, Tanaka A, Isono K, Kuhara S, Ogasawara N, Kikuchi H. Genome sequencing and analysis of *Aspergillus oryzae*. Nature 2005;438:1157-1161.
10. Machida M. Progress of *Aspergillus oryzae* genomics. Adv Appl Microbiol 2002;51:81-106.
11. Christensen T, Woeldike H, Boel E, Mortensen SB, Hjortshoej K, Thim L, Hansen MT. High level expression of recombinant genes in *Aspergillus oryzae*. Nat Biotech. 1988;6:1419-1422.
12. Gouka RJ, Punt PJ, van den Hondel CA. Efficient production of secreted proteins by *Aspergillus*: progress, limitations and prospects. Appl Microbiol Biotechnol. 1997;47:1-11.
13. Diaz-Godinez G, Soriano-Santos J, Augur C, Viniegra-Gonzalez G. Exopectinases produced by *Aspergillus niger* in solid-state and submerged fermentation: a comparative study. J Ind Microbiol Biotechnol 2001;26:271-275.
14. Elinbaum S, Ferreyra H, Ellenrieder G, Cuevas C. Production of *Aspergillus terreus* alpha-l-rhamnosidase by solid state fermentation. Lett Appl Microbiol. 2002;34:67-71.
15. Oda K, Kakizono D, Yamada O, Iefuji H, Akita O, Iwashita K. Proteomic analysis of extracellular proteins from *Aspergillus oryzae* grown under submerged and solid-state culture conditions. Appl Environ Microbiol. 2006;72:3448-57.
16. Hata Y, Ishida H, Ichikawa E, Kawato A, Suginami K, Imayasu S. Nucleotide sequence of an alternative glucoamylase-encoding gene (*glaB*) expressed in solid-state culture of *Aspergillus oryzae*. Gene 1998;207:127-134.
17. Ishida H, Hata Y, Kawato A, Abe Y, Suginami K, Imayasu S. Identification of functional elements that regulate the glucoamylase-encoding gene (*glaB*) expressed in solid-state culture of *Aspergillus oryzae*. Curr Genet. 200037:373-379.
18. Kitano H, Kataoka K, Furukawa K, Hara S. Specific expression and temperature-dependent expression of the acid protease-encoding gene (*pepA*) in *Aspergillus oryzae* in solid-state culture (rice-*koji*). J Biosci Bioeng. 2002;93:563-567.
19. Akao T, Gomi K, Goto K, Okazaki N, Akita O. Subtractive cloning of cDNA from *Aspergillus oryzae* differentially regulated between solid-state culture and liquid (submerged) culture. Curr Genet. 2002;41:275-281.
20. Yazawa H, Tokuoka M, Kozato H, Mori Y, Umeo M, Toyoura R, Oda K, Fukuda H, Iwashita K. Investigation of relationship between sake-making parameters and sake metabolites using a newly developed sake metabolome analysis method. J Biosci Bioeng. 2019;128:183-190.

21. Ito K, Kimizuka A, Okazaki N, Kobayashi S. Mycelial distribution in rice *Koji*. J Fermenta Bioeng. 1989;68:7-13. (in Japanese)
22. Ito K, Gomi K, Kariyama M, Miyake T. Quantitative evaluation of haze formation of *koji* and progression of internal haze by drying of *koji* during *koji* making. J Biosci Bioengin 2017;124:62-70.
23. Matsunaga K, Furukawa K, Hara S. Effects of enzyme activity on the mycelial penetration of rice *koji*. J Brew Soc Japan. 2002;97:721-726. (in Japanese)
24. Yanagiuchi T, Fukuda K, Nagano T, Nakamura S, Miyawaki M, Yoshifumi K, Wakai Y. Differences in the quality of sake *koji* made with various sake seed-*koji*: influences of various conditions on the making process of sake *koji*. J Brew Soc Japan 1993;88:559-564. (in Japanese)
25. Sudo S, Koseki T, Kizaki Y. Factors in the formation of haze. J Brew Soc Japan. 2002;97: 369-376. (in Japanese)
26. Wisman AP, Tamada Y, Hirohata S, Gomi K, Fukusaki E, Shimma S. Mapping *haze-komi* on rice *koji* grains using β-glucuronidase expressing *Aspergillus oryzae* and mass spectrometry imaging. J Biosci Bioeng. 2019; in print
27. Okuda M. Rice used for Japanese sake making. Biosci Biotechnol Biochem. 2019;83:1428-1441.
28. Bao J. Rice milling quality. Rice Chemistry and Technology (Fourth Edition). 2019; 339-369. published by Elsevier Inc. in cooperation with AACC International.
29. Anzawa Y, Nabekura Y, Satoh K, Satoh Y, Ohno S, Watanabe T, Kaneoke M, Kume K, Mizunuma M, Watanabe K, Katsumata K, Hirata D. Polishing properties of sake rice Koshitanrei for high-quality sake brewing. Biosci Biotechnol Biochem. 2013;77:2160-5.
30. Katayama T, Nakamura H, Zhang Y, Pascal A, Fujii W, Muruyama J. Forced recycling of an AMA1-based genome-editing plasmid allows for efficient multiple gene deletion/integration in the industrial filamentous fungus *Aspergillus oryzae*. Appl. Environ. Microbiol. 2019; 85:e01896-18.
31. Okabe T, Katayama T, Mo T, Mori N, Jin FJ, Fujii I, Iwashita K, Kitamoto K, Maruyama J. BiFC-based visualisation system reveals cell fusion morphology and heterokaryon incompatibility in the filamentous fungus *Aspergillus oryzae*, Sci. Rep. 2018;8:2922.
32. Kojima H, Hasegawa H, Magarifuchi T, Fukuda H. Observation of rice *koji* by confocal laser scanning microscopy. Seibutsu-Kogaku Kaishi. 1999;77:339-344. (in Japanese)
33. Yoshii M, Aramaki I. Microstructure of sake-*koji*. J Brew Soc Japan. 2001;96:806-813. (in Japanese)
34. Iwano K, Ito T, Hasegawa E, Takahashi K, Takahashi H, Nakazawa N. Influence of the variety of rice and polishing rate on Japanese sake *koji* making. J Brew Soc Japan. 2004;99:55-63. (in Japanese)
35. Yoshizawa K, Ishikawa Y. Characteristics of sake-rice and its treatments. J Brew Soc Japan. 1974;69:645-650. (in Japanese)
36. Shimizu H, Nakatani T, Okabe M, Mikami S, Iwano K. Influence of Acid Phosphatase and Phytase on Parallel Fermentation in Sake Brewing. J Brew Soc Japan. 1996;91:362-366. (in Japanese)
37. Yoshino-Yasuda S, hasegawa O, Iga Y, shiraishi Y, Wagu Y, Suzuki T, Sugimoto T, Kusumoto K, Kato M, Kitamoto N. Disruption and Overexpression of Acid Phosphatase Gene (aphA) from a Miso *Koji*

Mold, *Aspergillus oryzae* KBN630, and Characterization of the Gene Product. Food Sci Technol Res. 2012;18:59-65.

38. Uehigashi H, Katou R, Moriyama H, Hoki Y, Nagata S, Ito S, Kamiya M. Effect of thiamine on Ginjou-shu brewing. J Brew Soc Japan. 2014;109:310-317. (in Japanese)
39. Ghosh S, Datta K, Datta SK. Rice vitamins. Rice Chemistry and Technology (Fourth Edition). 2019; 195-220. published by Elsevier Inc. in cooperation with AACC International.
40. Etxebeste O, Garzia A, Espeso EA, Ugalde U. *Aspergillus nidulans* asexual development: making the most of cellular modules. Trends Microbiol. 2010;18:569-76.
41. Tanaka M, Yoshimura M, Ogawa M, Koyama Y, Shintani T, Gomi K. The C2H2-type transcription factor, FlbC, is involved in the transcriptional regulation of *Aspergillus oryzae* glucoamylase and protease genes specifically expressed in solid-state culture. Appl Microbiol Biotechnol. 2016;100:5859-68.
42. Maruyama J, Nakajima H, Kitamoto K. Visualization of nuclei in *Aspergillus oryzae* with EGFP and analysis of the number of nuclei in each conidium by FACS. Biosc Biotech Biochem. 2001;65:1504-1510.
43. Ishi K, Maruyama J, Juvvadi PR, Nakajima H, Kitamoto K. Visualizing nuclear migration during conidiophore development in *Aspergillus nidulans* and *Aspergillus oryzae*: multinucleation of conidia occurs through direct migration of plural nuclei from phialides and confers greater viability and early germination in *Aspergillus oryzae*. Biosc Biotech Biochem. 2005;69:747-754.
44. Clutterbuck AJ. Synchronous nuclear division and septation in *Aspergillus nidulans*. J Gen Microbiol. 1970;60:133-135.
45. Suelmann R, Sievers N, Fischer R. Nuclear traffic in fungal hyphae: *in vivo* study of nuclear migration and positioning in *Aspergillus nidulans*. Mol Microbiol. 1997;25:757-69.
46. De Souza CP, Osmani AH, Hashmi SB, Osmani SA. Partial nuclear pore complex disassembly during closed mitosis in *Aspergillus nidulans*. Curr Biol. 2004;14:1973-84.
47. Toews MW, Warmbold J, Konzack S, Rischitor P, Veith D, Vienken K, Vinuesa C, Wei H, Fischer R. Establishment of mRFP1 as a fluorescent marker in *Aspergillus nidulans* and construction of expression vectors for high-throughput protein tagging using recombination in vitro (GATEWAY). Curr Genet. 2004;45:383-9.
48. Suresh S, Markossian S, Osmani AH, Osmani SA. Nup2 performs diverse interphase functions in *Aspergillus nidulans*. Mol Biol Cell. 2018;29:3144-3154.
49. Suresh S, Markossian S, Osmani AH, Osmani SA. Mitotic nuclear pore complex segregation involves Nup2 in *Aspergillus nidulans*. J Cell Biol. 2017;216:2813-2826.
50. Minke PF, Lee IH, Plamann M. Microscopic analysis of *Neurospora* ropy mutants defective in nuclear distribution. *Fungal Genet. Biol.*1999;28:55–67.
51. Gladfelter AS, Hungerbuehler AK, Philippsen P. Asynchronous nuclear division cycles in multinucleated cells. J Cell Biol. 2006;172:347-62.

52. Bertoli C, Skotheim JM, de Bruin RA. Control of cell cycle transcription during G1 and S phases. Nat Rev Mol Cell Biol. 2013;14:518-28.

Table

Table 1.

Function	Gene (relative)	Y50/Y90
a-amylase, glucoamylase	*amyA-C, glaA*	5.2, 1.7
acid protease	*pepA*	0.08
fatty acid synthase	*fasA, fasB*	5.6, 7.4
delta-9-stearic acid desaturase	*sdeA, sdeB*	13.7, 20.2
phytase	*phyA*	4.4
acid phosphatase	*aphA, pacA,phoA*	2.0, 1.6, 1.6
alkaline phosphatase	*pho8*	5.8
thiamine synhtesis	*thiA, thi6*	4.9, 3.9
biotin synhtesis	*bioF, bioA*	6.9, 3.2
pantotate synhtesis	*apbA, panB*	4.9, 3.0
conidiophore development, solid state culture regulation	*flbA, flbB, flbD, brlA* *flbC*	8.0, 1.6, 2.5, 2.4 4.7

Figures

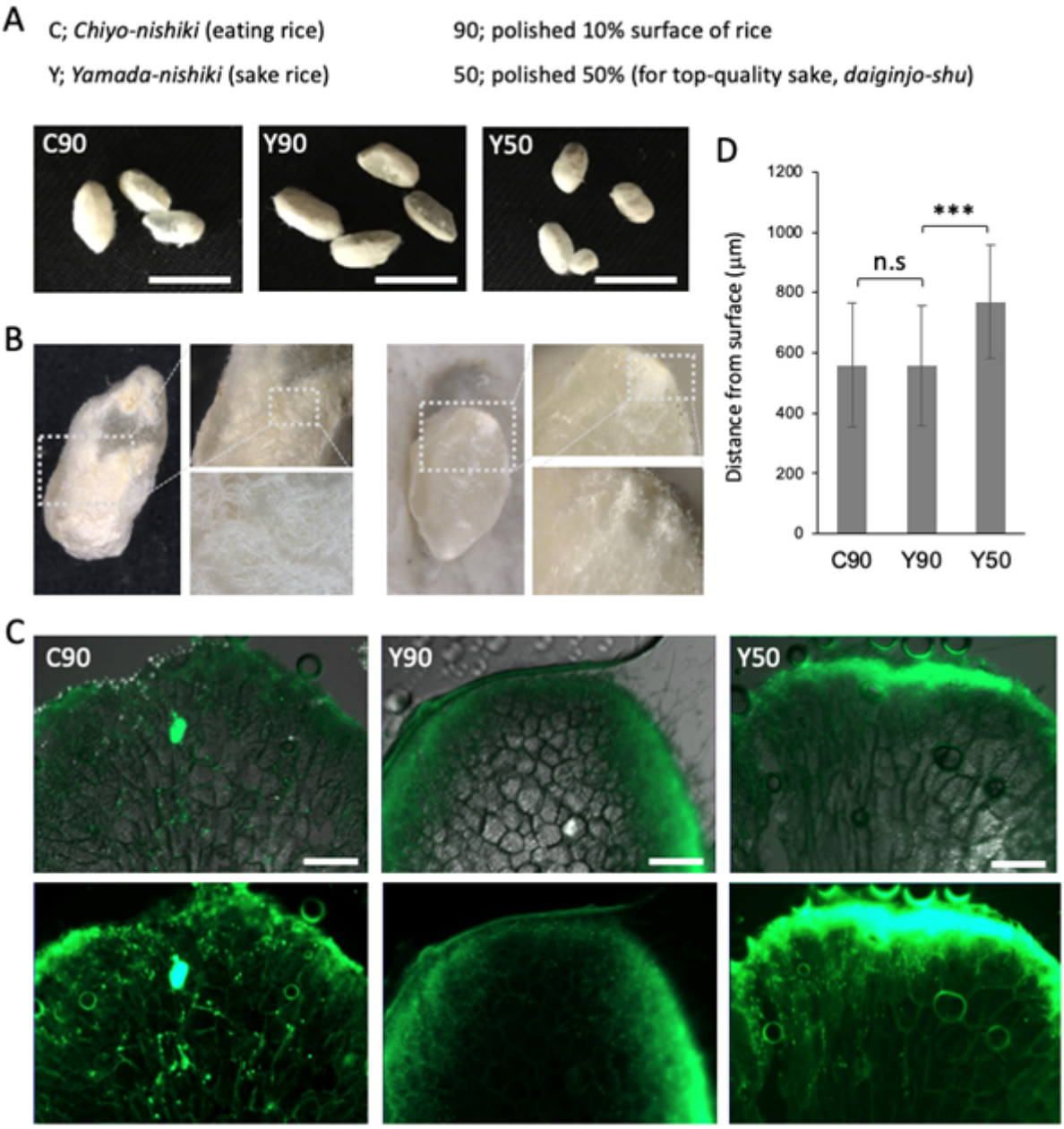

Figure 1

Imaging analysis of A. oryzae penetration into steamed rice. (A) Koji of different rice races and polishing rates. Chiyo-nishiki (eating rice) and Yamada-nishiki (sake rice) polished 90% or 50%. Scale bar: 1 cm. (B) Images of section of koji by zoom microscopy. (C) Fluorescent images of A. oryzae (H2B-GFP) penetration into the steamed rice. The sections were sliced by cryo-microtome. Scale bars: 200 □m. (D) Distance of fungal penetration from surface in C90, Y90 and Y50. Error bar: S.D., n = 20 hyphae in 3 independent koji. *** P < 0.001.

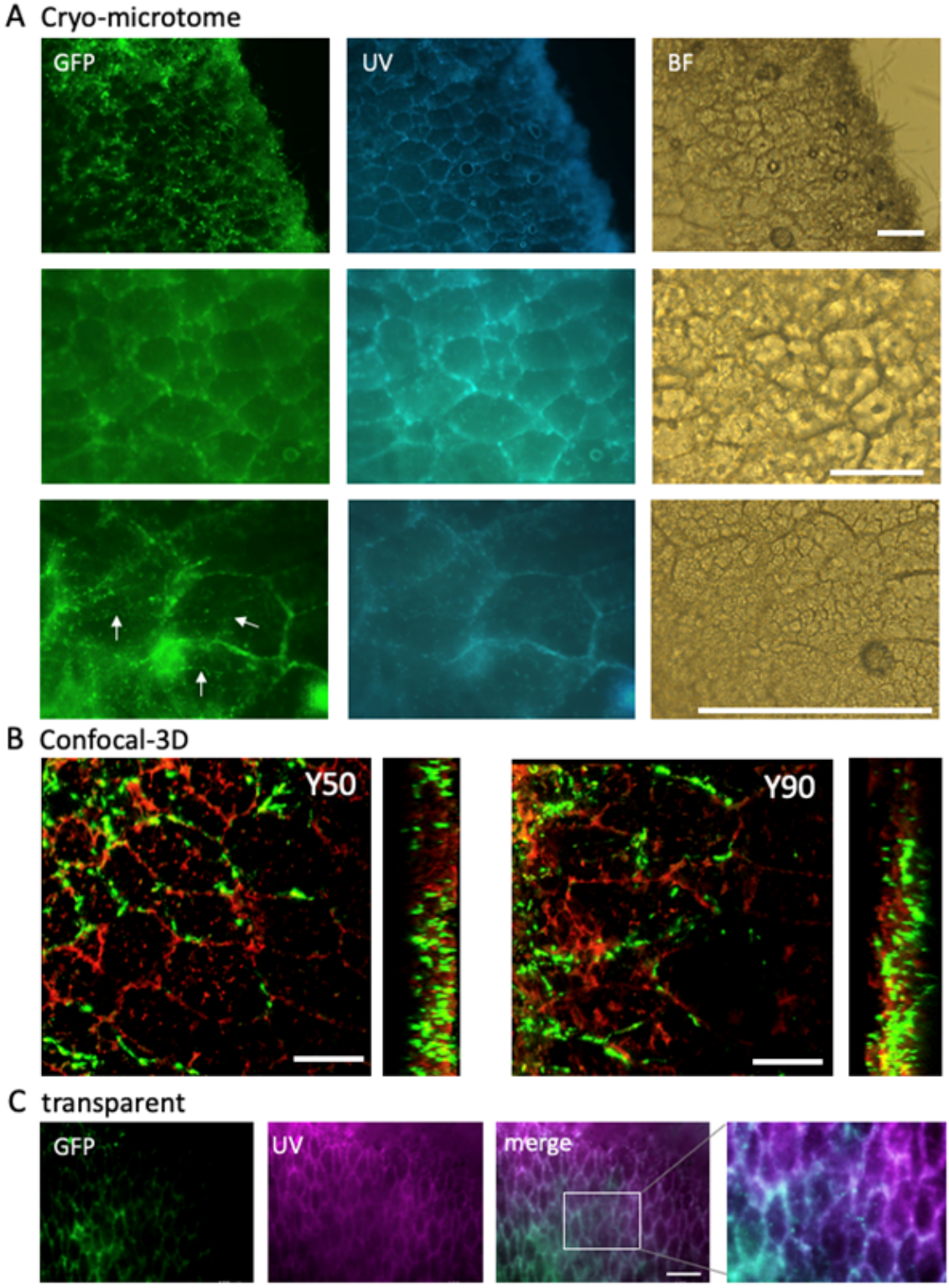

Figure 2

Fluorescent imaging analysis of A. oryzae penetration inter-rice cells and intra-rice cells. (A) Fluorescent images of A. oryzae (H2B-GFP) penetration inter-rice cells and intra-rice cells in Y50. The rice cells were shown by UV and BF (bright field). The sections were sliced by cryo-microtome. Hyphal growth inside of rice cells was indicated by arrows. Scale bars: 50 □m. (B) Confocal-3D imaging of the koji section from Y50 and Y90. A. oryzae (green), rice cells visualized by the autofluorescence (red). See also Movies 1 and

2. Scale bars: 50 m. (C) The koji treated with the transparent reagent were imaged by fluorescent microscopy. A. oryzae (green), rice cells (purple). Scale bar: 100 m.

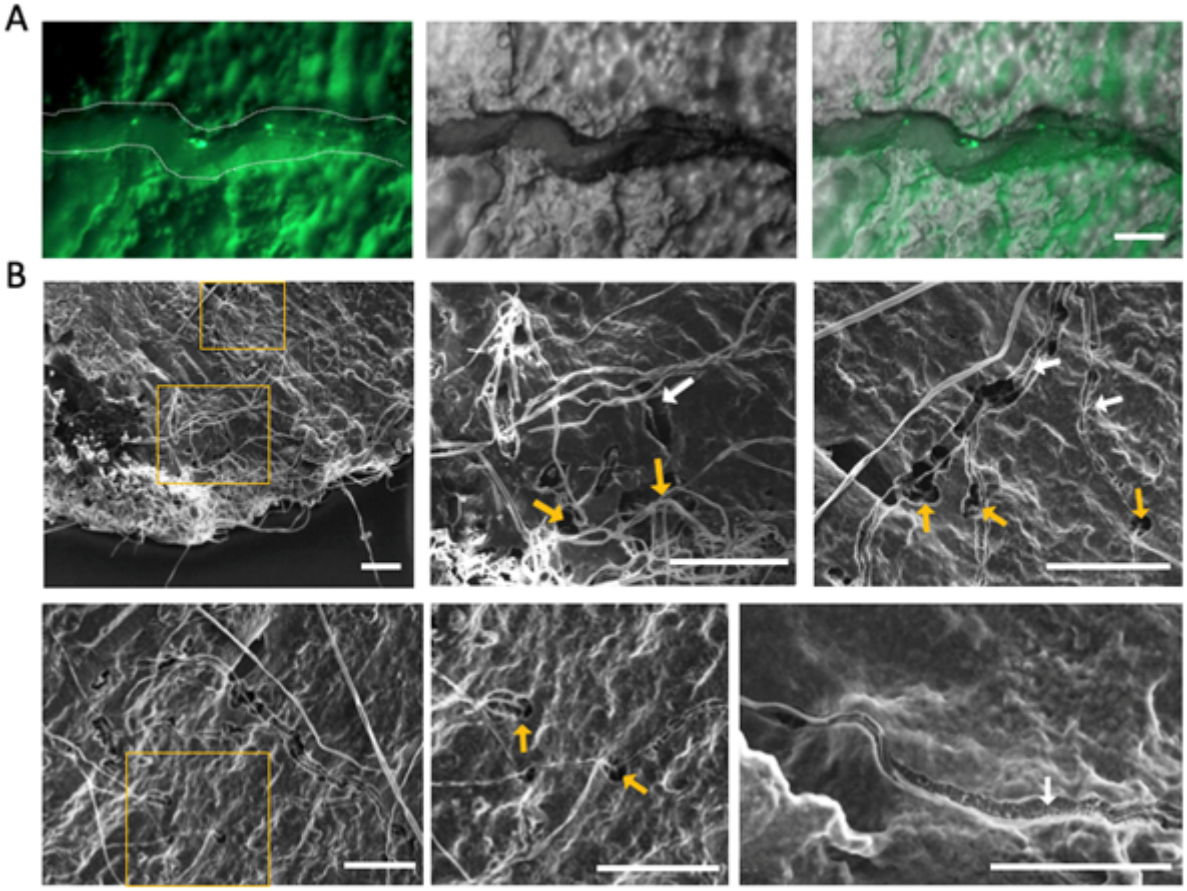

Figure 3

Fluorescent and SEM imaging analyses of A. oryzae penetration intra-rice cells. (A) Fluorescent images of A. oryzae (H2B-GFP) penetration intra-steamed rice Y50. Hyphal growth through surrounding space like a furrow in the rice (arrow and dotted line). Scale bars: 20 m. (B) SEM images of the koji section. Scale bars: 100 m. Cross sections of hyphae from or to holes (yellow arrows). Vertical sections of hyphae surrounding space like a furrow (white arrows).

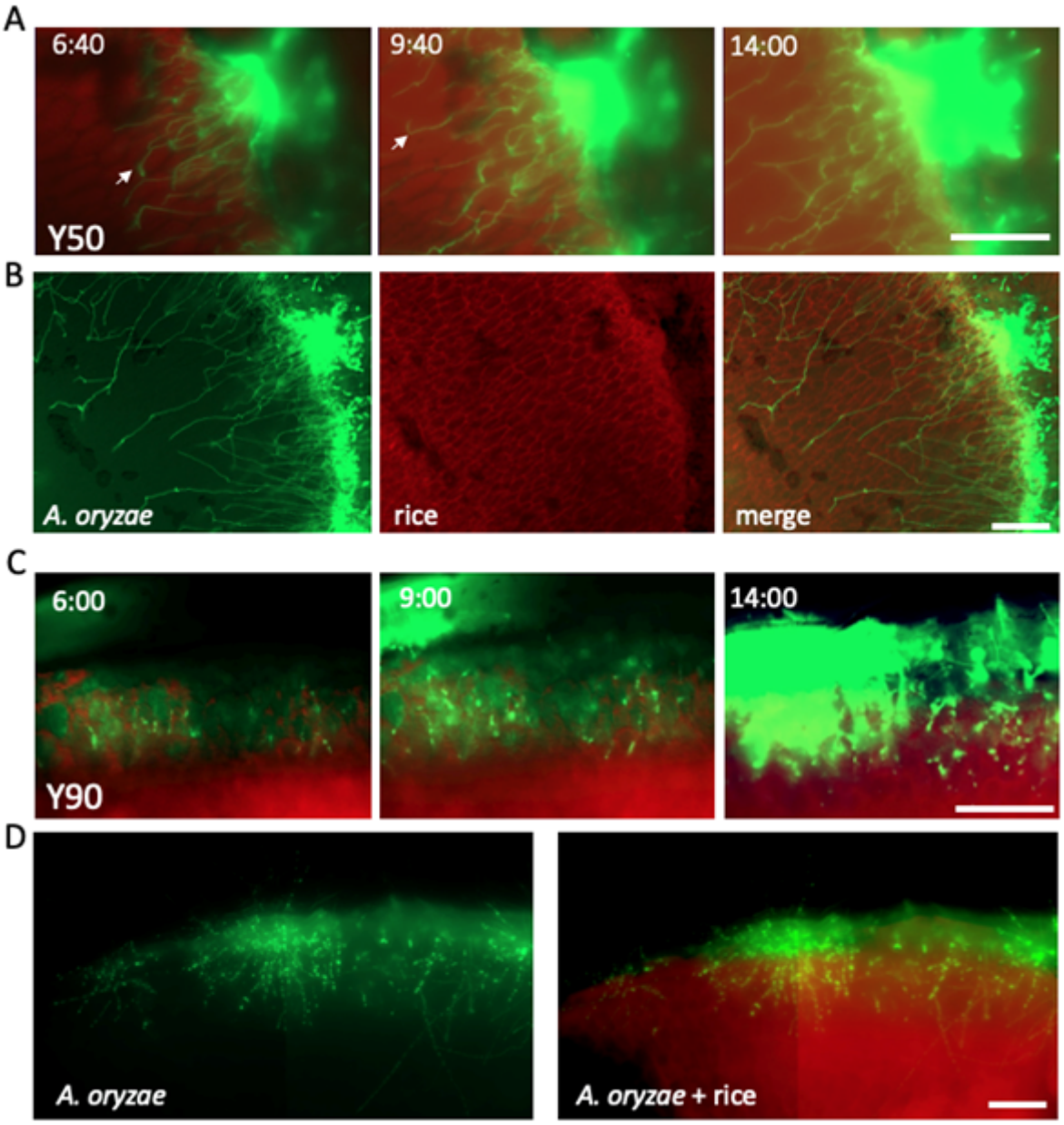

Figure 4

Time-lapse imaging analysis of A. oryzae penetration into steamed rice. The sections of koji Y50 (A, B) and Y90 (C, D), A. oryzae (green), rice cells (red), were imaged every 10 or 20 minutes for 14 hours by fluorescent microscopy. See also Movie 3 and 4. Time-lapse images (A, C) and broader images at 14 hours (B, D). (A). Some hyphae changed the growth direction after hitting the rice cell shape (arrows). Scale bars: 200 □m.

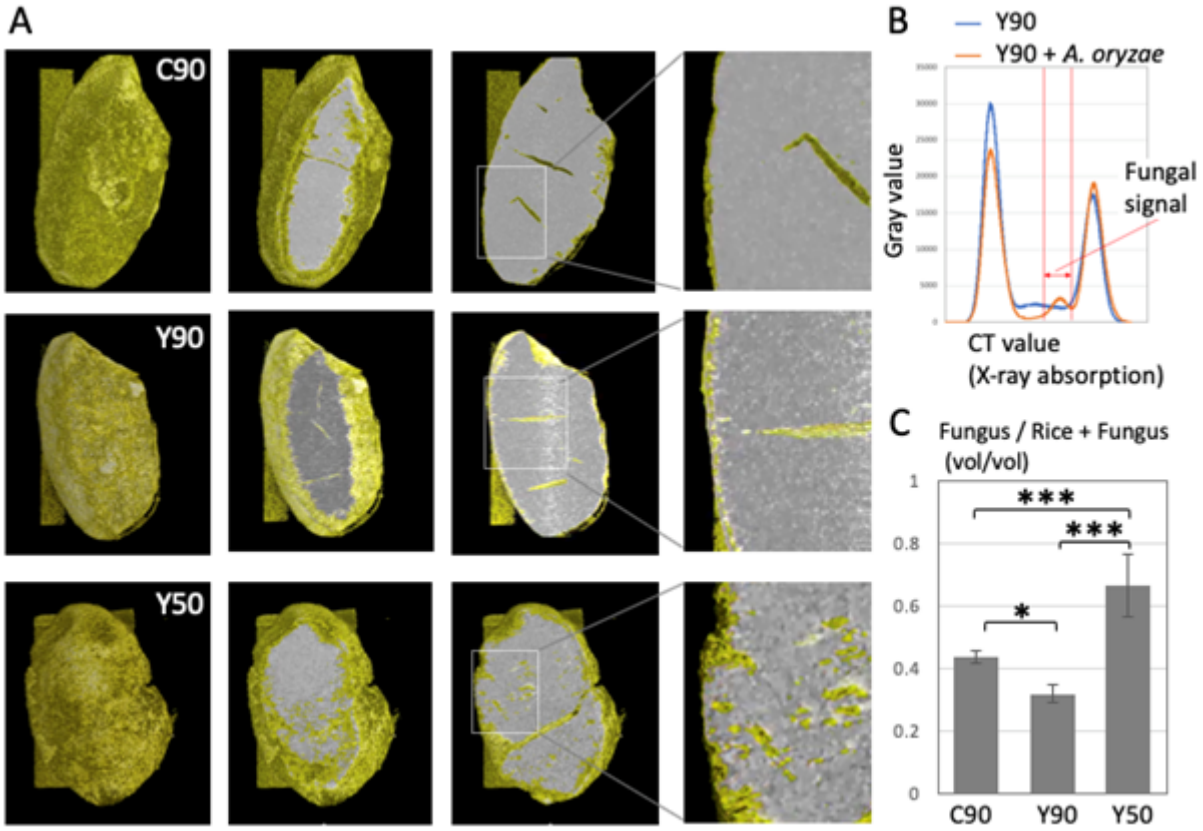

Figure 5

X-ray CT analysis of A. oryzae penetration into steamed rice. (A) Image sequence of X-ray CT analysis in C90, Y90 and Y50. See also Movie 5-7. The rice and fungus are shown in white and yellow, respectively. (B) The fungal signals were determined by the peak in CT value (X-ray absorption) only found in Y90 + A. oryzae. (C) Fungal volume was calculated from the 3D data. Error bar: S.D., n = 3. * P< 0.05, *** P < 0.001.

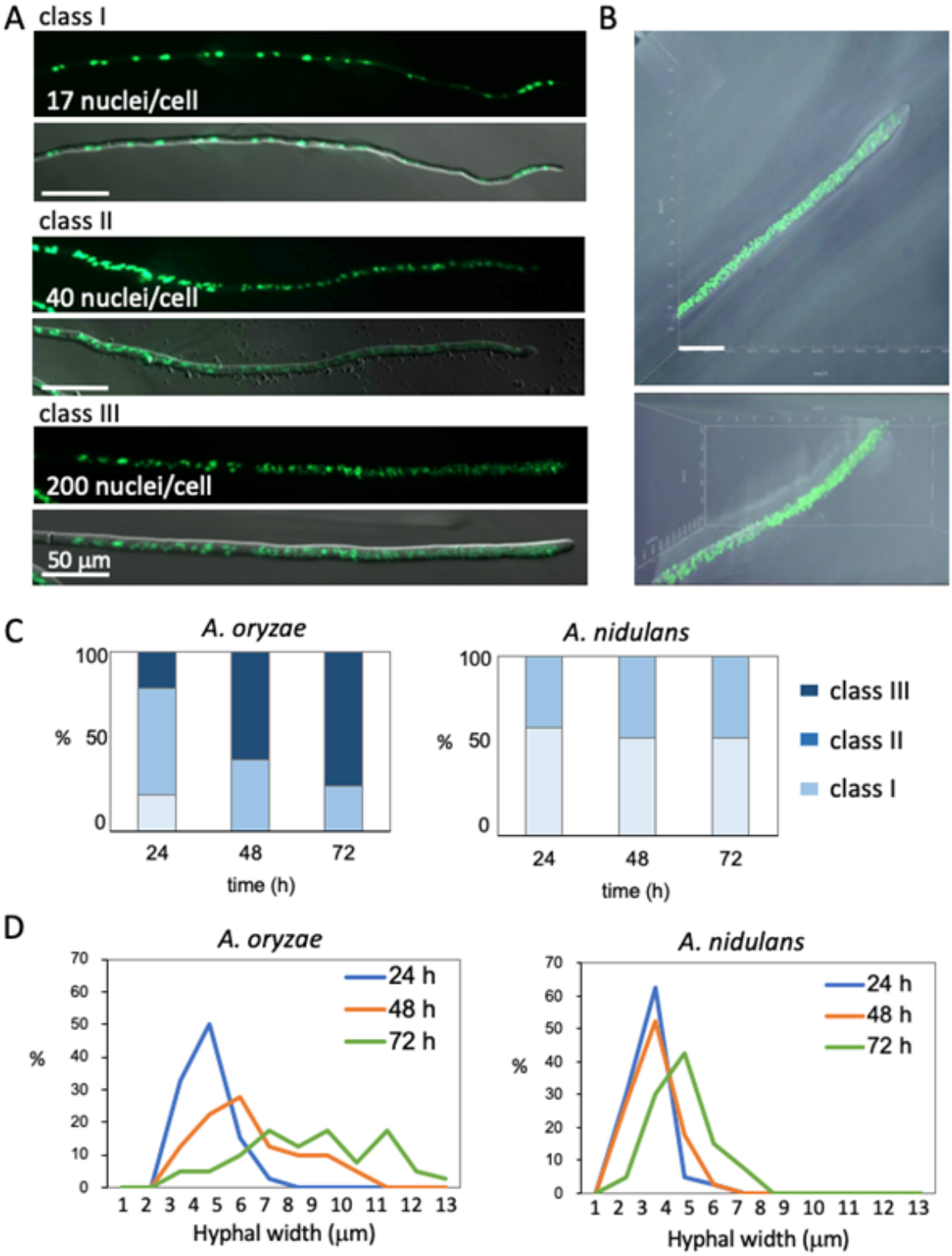

Figure 6

Increase of nuclear number in A. oryzae but not in A. nidulans. (A) Images of nuclei in the tip compartment of A. oryzae. The septal positions are shown by arrows. Scale bars: 50 µm. (B) Confocal-3D imaging of nuclei in the A. oryzae tip compartment. See also Movie 8. Scale bar: 40 µm. (C) Ratio of nuclear distribution pattern classified as class I, II, III (A) in A. oryzae (left) and A. nidulans (right) at 24-,

48- and 72-hours growth (n = 20). (D) Ratio of hyphal width in A. oryzae (left) and A. nidulans (right) at 24-, 48- and 72-hours growth (n = 100).

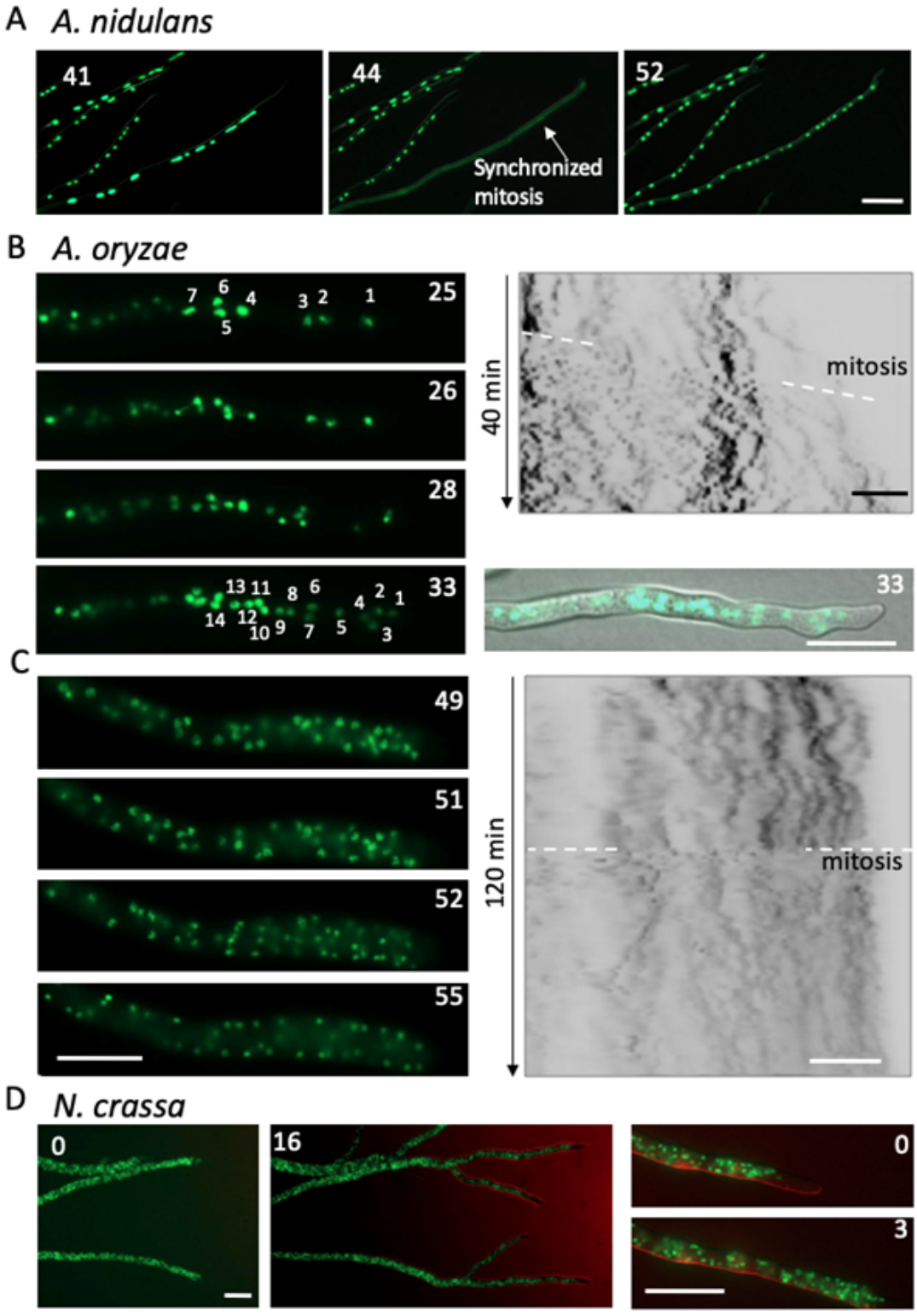

Figure 7

Nuclear distribution and mitosis in A. nidulans, A. oryzae and N. crassa. (A) Image sequence of synchronized mitosis in A. nidulans observed every minute for 3 hours by fluorescent microscopy. See also Movie 9. (B, C) Image sequence of nuclei in the A. oryzae tip compartment from 1 day incubation

(Movie 10) and 3 days incubation (Movie 11). Kymographs of nuclear distribution along the hypha. (D) Image sequence of nuclei in N. crassa from Movie 12, 13. The elapsed time is given in minutes (A-D). (A-C) Scale bars: 20 □m, (D) Scale bars: 50 □m.

Supplementary Files

This is a list of supplementary files associated with this preprint. Click to download.

- Movie7Y50CT.mov
- Movie8Aonuc3D.avi
- Supplementaryfigure13.pdf
- Movie3Y50t.avi
- Movie11Aomitosis2.avi
- Movie12Nct1.avi
- Movie6Y90CT.mov
- Movie10Aomitosis.avi
- Movie5C90CT.mov
- Supplementtable.xlsx
- Movie1Y503D.mov
- Movie2Y903D.mov
- Movie4Y90t.avi
- Movie9Ant.avi
- Movie13Nct2.avi